Apoptosis of Ocular Surface Cells in Experimentally Induced Dry Eye

Steven Yeh,[1] *Xiu Jun Song,*[1,2] *William Farley,*[1] *De-Quan Li,*[1] *Michael E. Stern,*[3] *and Stephen C. Pflugfelder*[1]

Purpose. To evaluate to effect of experimental dry eye on ocular surface apoptosis.

Methods. Aqueous tear production and clearance were inhibited by systemic administration of scopolamine and exposure to an air draft for 12 days in 4- to 6-week-old 129SvEv/CD-1 mixed white mice. Eyes and ocular adnexa were excised, cryosectioned, and evaluated for apoptosis by terminal deoxynucleotidyl transferase-mediated dUTP-digoxigenin nick end labeling (TUNEL) assay, immunohistochemical assay for caspase-3 and poly(ADP-ribose) phosphate (PARP), and examination of nuclear morphologic changes by Hoechst DNA nuclear staining and transmission electron microscopy.

Results. The number of TUNEL-positive cells in the mice with induced dry eye was significantly increased compared with control mice in the following ocular regions: central corneal ($P < 0.0014$), peripheral corneal ($P < 0.0001$), bulbar conjunctival ($P < 0.0021$), and tarsal conjunctival ($P < 0.0046$) epithelia; tarsal conjunctival stroma ($P < 0.0274$); and lid margin ($P < 0.0219$, $n = 4$ in all cases). There were no significant differences observed between treated and control groups in the central corneal, peripheral corneal, or bulbar conjunctival stroma; meibomian glands; skin; retina-choroid; or episcleral regions. Immunohistochemistry for caspase-3 and poly(ADP-ribose) polymerase p85 fragment revealed increased immunoreactivity in regions of increased TUNEL positivity, particularly in the corneal and conjunctival epithelial cells. Ultrastructural morphologic changes consistent with apoptosis were observed in the conjunctival epithelial cells.

Conclusions. Experimentally induced dry eye in mice causes apoptosis of cells in ocular surface tissues including the central and peripheral corneal epithelium, bulbar and tarsal conjunctival epithelia, tarsal conjunctival stroma, and lid margin. Apoptosis may play a key role in the pathogenesis of keratoconjunctivitis sicca and may be a therapeutic target for this condition. (*Invest Ophthalmol Vis Sci.* 2003;44:124–129) DOI: 10.1167/iovs.02-0581

From the [1]Ocular Surface Center, Cullen Eye Institute, Baylor College of Medicine, Department of Ophthalmology, Houston, Texas; [3]Allergan, Inc., Irvine, California; and the [2]Third Hospital of Hebei Medical University, Shijiazhuang, China.

Supported in part by Allergan, Inc, an unrestricted grant from Research to Prevent Blindness, The Oshman Foundation, and The William Stamps Farish Fund.

Submitted for publication June 13, 2002; accepted July 30, 2002.

Disclosure: **S. Yeh**, None; **X.J. Song**, None; **W. Farley**, None; **D.-Q. Li**, None; **M.E. Stern**, Allergan, Inc. (E); **S.C. Pflugfelder**, Allergan, Inc. (C, F)

The publication costs of this article were defrayed in part by page charge payment. This article must therefore be marked "*advertisement*" in accordance with 18 U.S.C. §1734 solely to indicate this fact.

Corresponding author: Stephen C. Pflugfelder, Baylor College of Medicine, 6565 Fannin, NC-205 Ocular Surface Center, Houston, TX 77030; stevenp@bcm.tmc.edu.

Dysfunction of the integrated ocular surface–lacrimal gland functional unit causes the ocular surface disease keratoconjunctivitis sicca (KCS).[1] The ocular surface in this condition is poorly lubricated because of decreased production of mucins by the stratified epithelia and conjunctival goblet cells and has altered barrier function manifesting clinically as increased permeability to fluorescein dye.[2] Instability of the precorneal tear film and punctate epitheliopathy cause blurred and fluctuating vision. The cause of these pathologic changes is currently unknown; however, there is mounting evidence that inflammation may play an important role.

Evidence for immune-based inflammation in dry eye includes increased density of inflammatory cells and elevated levels of inflammatory cytokines[3–5] and proapoptotic factors[6–9] in the ocular surface and tear film. The relationship between ocular surface inflammation and apoptosis has also been the subject of much investigation. Expression of proapoptotic markers (Fas, Fas ligand, APO2.7, CD40, and CD40 ligand) by the conjunctival epithelium in KCS has been found to be significantly higher than in normal eyes and is positively correlated with expression of HLA-DR class II antigen, an immune activation marker.[6,7] After 6 months of therapy with cyclosporin A , the levels of cell membrane markers for apoptosis (i.e., Fas) and inflammation, such as HLA-DR, were significantly reduced.[8]

In studies of chronic idiopathic canine KCS, increased apoptosis was observed in epithelial cells and decreased apoptosis in lymphocytes in the conjunctiva and lacrimal glands.[9] Immunohistochemistry studies demonstrated that p53, Fas, and Fas ligand were elevated in lacrimal acinar cells and conjunctival epithelial cells in dogs with dry eye.[9] In contrast, low levels of expression of Bcl-2, an antiapoptosis marker, was observed in these tissues. After treatment with topical cyclosporin A, induction of apoptosis in lymphocytes and suppression of apoptosis in conjunctival epithelial cells was observed in these animals.[9] In lacrimal acinar cells, a decrease in p53 and an increase in Bcl-2 was also observed after treatment with cyclosporin A.[9]

Although apoptosis has been demonstrated in chronic dry eye in humans and dogs, no studies have been undertaken to evaluate the occurrence and kinetics of apoptosis on the ocular surface after acute induction of dry eye. We investigated whether apoptosis develops on the ocular surface after experimental induction of dry eye in a mouse model of KCS, using three different techniques: the TUNEL assay, which detects DNA fragmentation; immunodetection of two cellular markers of apoptosis: activated caspase-3 (a downstream effector protease) and cleaved poly(ADP-ribose) polymerase (PARP; a nuclear DNA-binding protein); and examination of cell nuclei for morphologic changes characteristic of apoptosis by nuclear staining with a DNA-binding dye, and transmission electron microscopy.

TABLE 1. Quantitation of TUNEL-Positive Ocular Surface Cells

Ocular Surface Tissue	Dry Eye Mice (n = 4)	Untreated Mice (n = 4)	P
Central corneal epithelium	32.5 ± 9.7	3.75 ± 3.4	<0.0014*
Central corneal stroma	3.75 ± 4.5	1.0 ± 0.82	<0.3893
Peripheral corneal epithelium	28.0 ± 6.2	0.25 ± 0.50	<0.0001*
Peripheral corneal stroma	3.25 ± 3.4	0.25 ± 0.50	<0.1317
Bulbar conjunctive epithelium	31.3 ± 11	2.75 ± 2.5	<0.0021*
Bulbar conjunctive stroma	5.0 ± 1.8	2.25 ± 1.7	<0.0701
Tarsal conjunctive epithelium	55.8 ± 25	0.5 ± 1.0	<0.0046*
Tarsal conjunctive stroma	4.25 ± 2.2	0.75 ± 0.96	<0.0274*
Lid margin	27.5 ± 15	4.0 ± 2.2	<0.029*
Meibomian glands	29.3 ± 25	0.75 ± 1.5	<0.0615
Skin	24.8 ± 22	3.75 ± 2.5	<0.1017
Retinal choroid	1.25 ± 1.3	0.5 ± 1.0	<0.3867
Episclera	0.50 ± 1.0	0.5 ± 1.0	<1.000

Values are mean ± SD. Probabilities by *t*-test.
* Indicates statistical significance ($P < 0.05$).

MATERIALS AND METHODS

Animal Treatment and Tissue Collection

All animal research protocols were approved by the Baylor College of Medicine Center for Comparative Medicine and conformed to the standards in the ARVO Statement for the Use of Animals in Ophthalmic and Vision Research.

Aqueous tear production and clearance were inhibited by subcutaneous injection of scopolamine (1 mg in 0.2 mL) three times daily in the flanks of 4- to 6-week-old 129SvEv/CD-1 white mice. Dry eye was induced in mice with a modification of a previously described technique.[10] Mice were exposed to a continuous air draft from a fan placed 6 in. in front of the cage in an environmentally controlled room (50% humidity, 18°C) for 10 hours a day for 12 consecutive days. These treatments cause a statistically significant decrease in aqueous tear production and tear clearance that results in increased corneal epithelial permeability to fluorescein dye, conjunctival squamous metaplasia, and loss of goblet cells.[10]

Mice were killed and their eyes and adnexa were excised, embedded in optimal cutting temperature (OCT) compound (VWR, Swannee, GA), flash frozen in liquid nitrogen, and sectioned with a cryostat (HM 500; Micron, Waldorf, Germany) into 5-μm sagittal slices that were placed on microscope slides (Superfrost/Plus; Fisher, Houston, TX). These were stored at −80°C until they were used in the studies of apoptosis.

Apoptosis Evaluation

A combination of immunohistochemical and morphologic studies were used to study apoptosis in our mouse model. Specifically, assays for DNA fragmentation (TUNEL), caspase 3 activation, and PARP cleavage were performed for immunohistochemical characterization of apoptosis; transmission electron microscopy and Hoechst dye nuclear staining were used for morphologic characterization of nuclear changes observed in apoptosis.

The terminal deoxynucleotidyl transferase-mediated dUTP-nick end labeling (TUNEL) assay, which detects 3′ hydroxyl ends in fragmented DNA as an early event in the apoptotic cascade,[11] was performed with a kit (ApopTag; Intergen Co., Purchase, NY), using a modification of the manufacturer's protocol as previously described.[11,12] Cryosections of whole mouse eyes were fixed in 1% paraformaldehyde, and cell membranes were permeabilized with 2:1 ethanol:acetic acid solution. The samples were incubated with TdT enzyme and 11-digoxigenin dUTP at 37°C for 90 minutes. After quenching the reaction, samples were blocked with blocking solution and incubated with anti-digoxigenin FITC-conjugated antibody for 60 minutes at room temperature. One cryosection was incubated with 1 μg/mL DNase I in TdT buffer for 30 minutes at room temperature before incubation with TdT enzyme and 11-digoxigenin dUTP as a positive reaction control.

After completion of the initial TUNEL procedure, the cryosections were evaluated for expression of activated caspase-3. After three washes in phosphate-buffered saline (PBS, pH 7.2), tissue samples were incubated with 5 μg/mL polyclonal rabbit anti-active caspase-3 primary antibody (PharMingen, San Diego, CA) or PBS as a primary antibody negative control at 4°C overnight. Samples were then blocked with 10% goat serum for 30 minutes at room temperature and incubated with goat anti-rabbit conjugated antibody (Alexa Fluor 594; Molecular Probes, Eugene, OR) for 45 minutes at room temperature, followed by three washes in PBS. Nuclei were then counterstained using 0.5 μg/mL Hoechst 33342 dye (Sigma, St. Louis, MO) in approximately 30 μL mounting gel (Gel Mount; Fisher) and a 22 × 50-mm coverslip (Fisher) then applied.

Apoptotic cells in different regions of the ocular surface were assessed by epifluorescence microscope (Eclipse E400; Nikon, Garden City, NY) . Photographs at 400× magnification were taken of representative areas of the cornea, bulbar conjunctiva, and tarsal conjunctiva. All TUNEL-positive cells were counted in the conjunctiva in 100-μm length × 100-μm width areas in the sagittal sections and in the cornea in 100-μm length × 20-μm width areas in the sagittal sections. A Student's *t*-test was used to analyze statistical significance of the data collected.

Immunodetection of the PARP p85 fragment was performed by immunofluorescent staining of cryosections that were fixed in 100% methanol at 4°C for 10 minutes. After three washes in PBS, samples were blocked with 10% goat serum for 30 minutes at room temperature and incubated for 2 hours at room temperature with a 1:50 dilution of rabbit anti-mouse PARP p85 fragment antibody (Promega, Madison, WI) or PBS, as a primary antibody negative control. After three washes in PBS, samples were incubated with goat anti-rabbit conjugated antibody (Alexa Fluor 488; Molecular Probes) for 45 minutes at room temperature, followed by three washes in PBS and nuclei counterstaining with 0.5 μg/mL Hoechst 33342 dye (Sigma).

For transmission electron microscopy, the cornea and conjunctiva were excised from treated and control mice. The tissues were diced carefully into 1-mm cubes, to avoid crushing, and fixed in 3% glutaraldehyde buffered to pH 7.2 with 0.01 M piperazine-*N*,*N*′-bis(2-ethane sulfonic acid [PIPES]) for 1 hour. They were rinsed in buffer and postfixed in PIPES-buffered osmium tetroxide (pH 7.2) for 1 hour at room temperature, rinsed in several changes of distilled water, and dehydrated through a graded series of ethanol. The dehydrated tissues were incubated in two 45-minute changes of propylene oxide followed by a 1:1 mixture of propylene oxide and Spurr resin for 1.5 hours. The tissue pieces were then incubated in pure resin for 1.5 hours, after

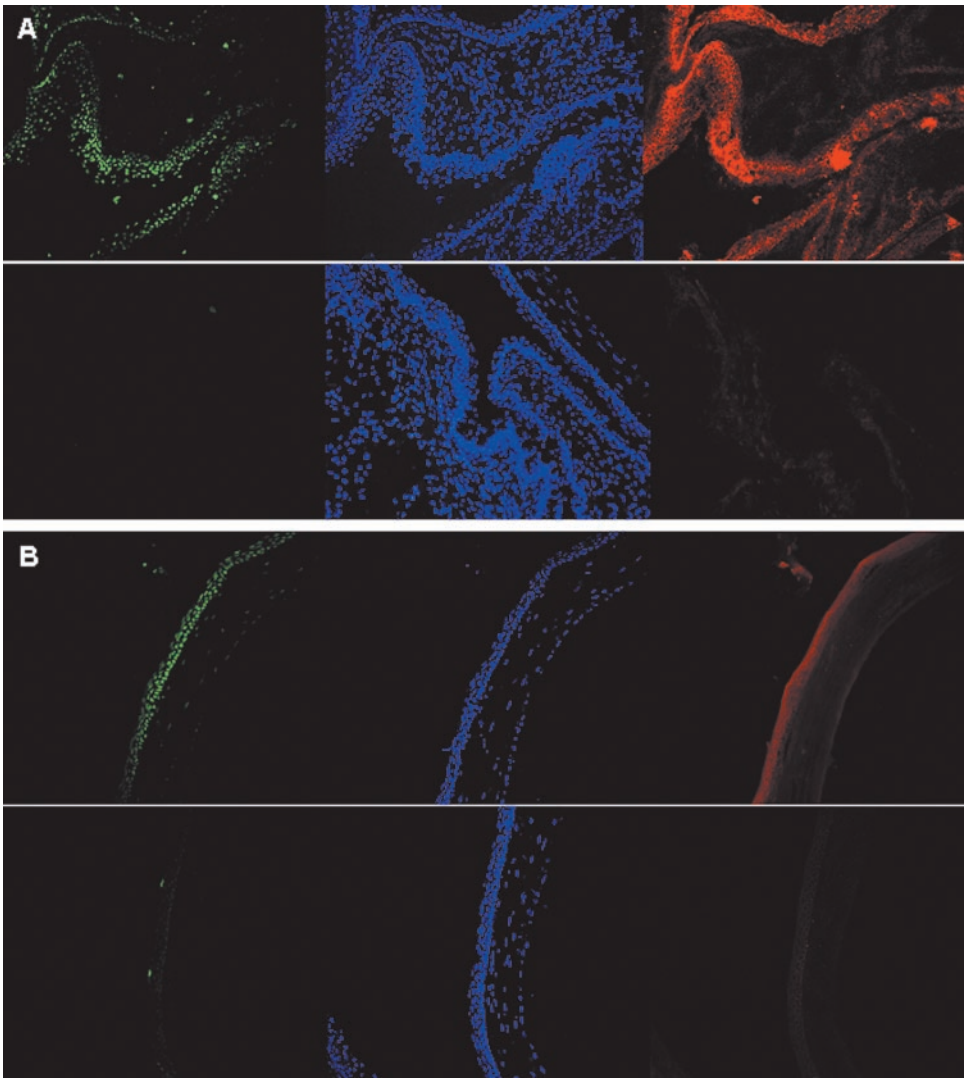

FIGURE 1. TUNEL-caspase-3 dual-label assay. In the conjunctiva (**A**) or cornea (**B**). (**A**) Conjunctiva. *Top left*: TUNEL-positive cells in bulbar conjunctival epithelium in treated mouse. *Top center*: Hoechst 33342 nuclear stain in treated mouse. *Top right*: active caspase-3 staining in treated mouse. *Bottom left*: TUNEL staining of bulbar and tarsal conjunctiva in untreated control mouse. *Bottom center*: Hoechst 33342 nuclear staining of bulbar and tarsal conjunctiva in untreated control mouse. *Bottom right*: active caspase-3 staining of bulbar and tarsal conjunctiva in untreated control mouse. (**B**) Central cornea. *Top left*: TUNEL-positive cells in central corneal epithelium in treated mouse. *Top center*: Hoechst 33342 nuclear stain in treated mouse. *Top right*: active caspase-3 staining of corneal epithelium in treated mouse. *Bottom left*: TUNEL-positive cells in superficial corneal epithelium of untreated control mouse. *Bottom center*: Hoechst 33342 nuclear stain in untreated control mouse. *Bottom right*: active caspase-3 staining in untreated control mouse.

which they were transferred to fresh resin in block molds and allowed to cure at 60°C overnight. Sections cut 1 μm thick from the hardened blocks were mounted on glass slides, stained with an alcoholic solution of toluidine blue and basic fuchsin and examined by light microscope. Areas of interest were trimmed, and 60-nm sections were cut and mounted on copper grids (300 mesh). The grids were stained with uranyl acetate and lead citrate and photographed with an electron microscope (model 100C Temscan; JEOL, Peabody, MA; and 4489 film; Eastman Kodak, Rochester, NY).

RESULTS

As previously reported, mice treated with systemic scopolamine injections and subjected to an air draft and desiccating environment showed a significant decrease in aqueous tear production and clearance by day 4 that was sustained throughout the treatment period.[10] Dryness was accompanied by development of KCS, with loss of conjunctival goblet cells and increased corneal epithelial permeability to carboxyfluorescein.[10] Apoptosis in the cornea and conjunctiva was assessed in mice treated in this fashion for 12 days and in untreated control animals.

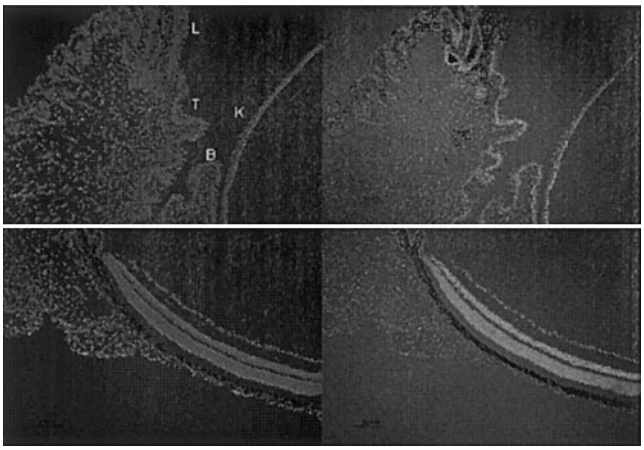

FIGURE 2. TUNEL assay positive control sections. *Top left*: Hoechst 33342 nuclear stain of lid margin (L), tarsal conjunctiva (T), bulbar conjunctiva (B), and cornea (K). *Top right*: TUNEL-positive cells in lid margin, tarsal and bulbar conjunctiva, and cornea. *Bottom left*: Hoechst 33342 nuclear stain of retina and choroid. *Bottom right*: TUNEL-positive cells of retina and choroid.

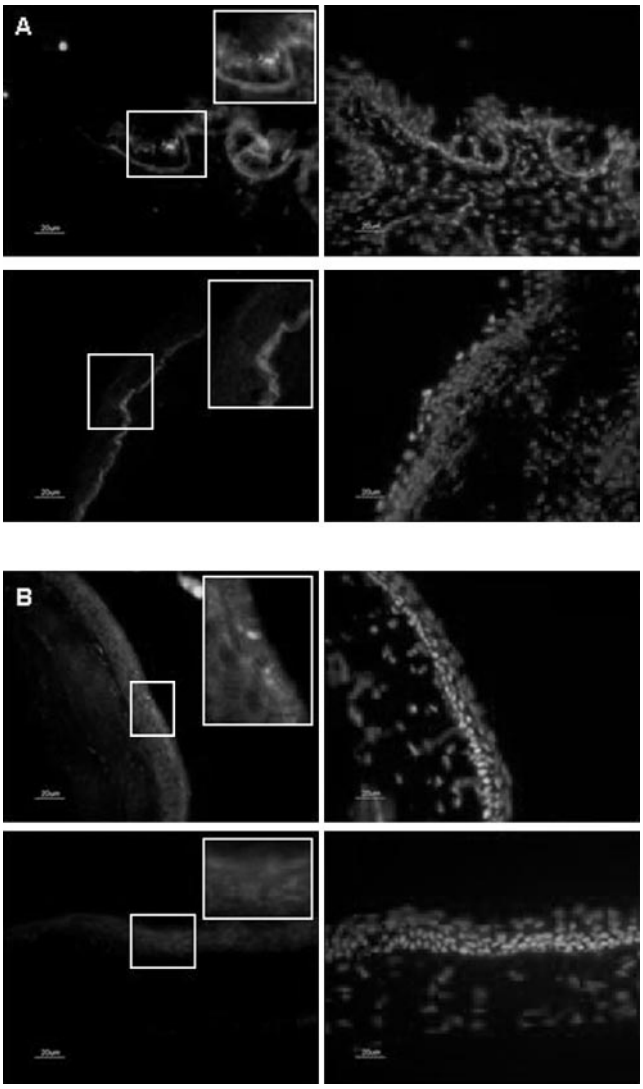

FIGURE 3. PARP staining of ocular surface tissues in the tarsal conjunctiva (**A**) and cornea (**B**). (**A**) Tarsal conjunctiva. *Top left*: numerous PARP-positive cells were detected in the superficial tarsal conjunctival epithelium of treated mouse. *Inset*: higher magnification of *boxed area* (*left*) highlights PARP-positive cells in conjunctival epithelium. *Top right*: Hoechst 33342 nuclear counterstain of tarsal conjunctival region. *Bottom left*: representative tarsal conjunctival section from untreated control mouse. *Inset*: higher magnification of *boxed area* (*left*) highlights absence of PARP-positive cells in conjunctiva of untreated control mouse *Bottom right*: Hoechst 33342 nuclear counterstain of tarsal conjunctiva in untreated control mouse. (**B**) Cornea. *Top left*: PARP-positive cells in superficial corneal epithelium of treated mouse. *Inset*: higher magnification of *boxed area* (*left*) highlights PARP-positive cells within the corneal epithelium. *Top right*: Hoechst 33342 nuclear counterstain of treated mouse cornea. *Bottom left*: PARP staining in cornea of untreated control mouse. *Inset*: higher magnification of *boxed area* (*left*) highlights absence of PARP-positive cells in cornea of untreated control mouse. *Bottom right*: Hoechst 33342 nuclear counterstain in cornea of untreated control mouse.

TUNEL and Caspase-3 Immunostaining

Normal, untreated control mice exhibited minimal apoptosis assessed by TUNEL staining in the cornea and conjunctiva (Table 1, Fig. 1). The number of TUNEL-positive cells was significantly increased in mice with induced dry eye compared with control mice in the following ocular surface tissues: central and peripheral corneal and bulbar and tarsal conjunctival epithelia; tarsal conjunctival stroma; and lid margin (Table 1, Fig. 1). There were no significant differences between dry eye and control groups in the central corneal, peripheral corneal, or bulbar conjunctival stroma; meibomian glands; skin; retina-choroid; or episcleral regions (Table 1).

Positive control experiments revealed TUNEL-positive cells throughout all regions of the eye including the cornea, bulbar and tarsal conjunctiva, retina, and choroid (Fig. 2).

Immunofluorescent staining for active caspase 3 revealed increased immunoreactivity in regions of TUNEL positivity.

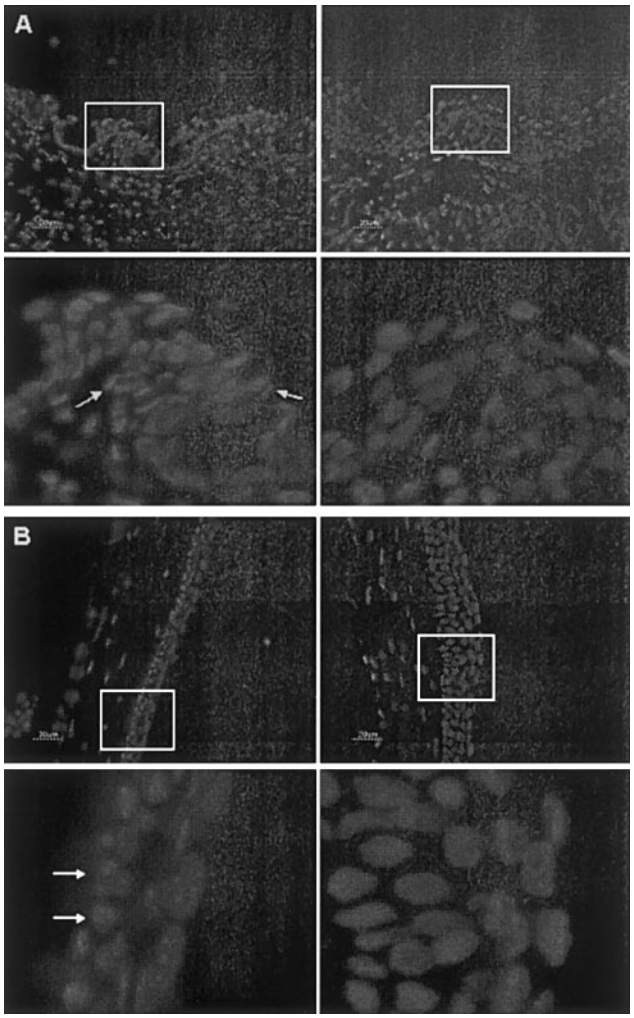

FIGURE 4. Hoechst 33342 nuclear stain of conjunctiva (**A**) and cornea (**B**). (**A**) Tarsal conjunctiva. *Top left*: the superficial tarsal conjunctival epithelium in the treated mouse showed dysmorphic architecture and small, fragmented appearance of nuclei. *Bottom left*: higher magnification of *boxed* area (*top left*) shows multiple fragmented cells in tarsal conjunctival epithelium of treated mouse (*arrows*). *Top right*: tarsal conjunctival architecture of untreated control mouse. *Bottom right*: higher magnification of *boxed* area (*top right*) shows no nuclear or cell fragments in the untreated mouse. (**B**) Cornea. *Top left*: the corneal epithelium in the treated mouse appeared thinned and atrophic with dysmorphic architecture. *Bottom left*: higher magnification of *boxed* area (*top left*) shows clumped chromatin in multiple basal epithelial cells (*arrows*). This finding was also seen to some degree in the superficial corneal epithelium. *Top right*: thicker, regular architecture in cornea of untreated control mouse. *Bottom right*: higher magnification of *boxed* area (*top right*) shows peripheral clumping of nuclear material, which was not seen to the same degree in the untreated control cornea as in the treated cornea.

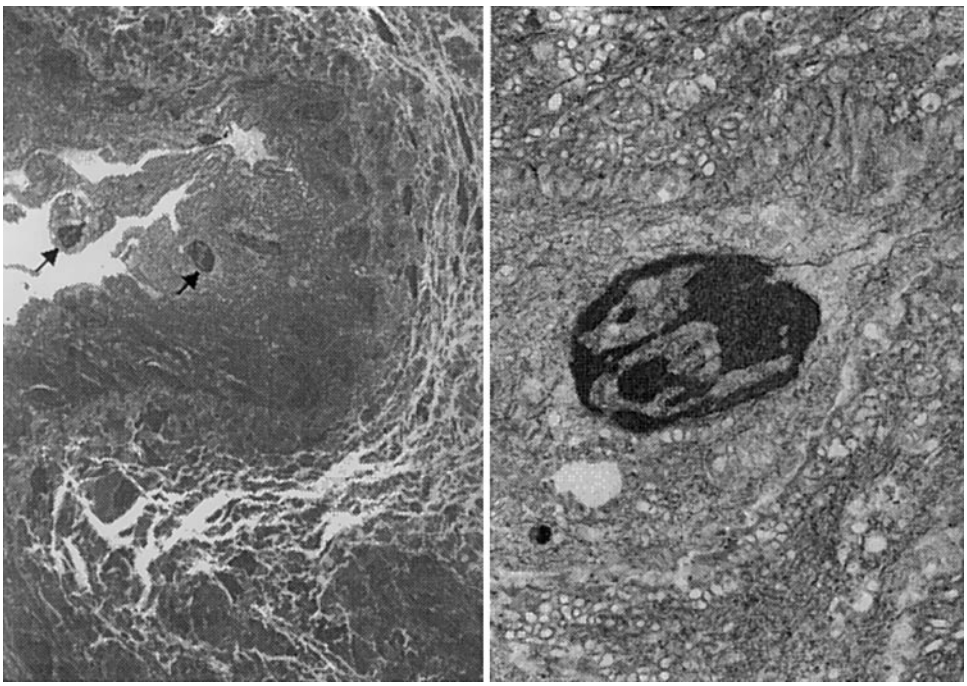

FIGURE 5. Transmission electron microscopy (TEM) of conjunctival epithelium of treated mouse. (**A**) Lower magnification TEM of bulbar conjunctiva epithelium. Multiple epithelial cells (*arrows*) exhibited chromatin condensation and peripheral aggregation of compacted chromatin. (**B**) Higher magnification TEM of bulbar conjunctiva epithelial cell showing chromatin condensation and peripheral aggregation of nuclear material, suggesting apoptotic cell death.

Specifically, active caspase 3 activity was localized to the central corneal epithelium, peripheral corneal epithelium, superficial conjunctival epithelium, and lid margins of the mouse with induced dry eye. This staining was not observed in the negative control for which secondary antibody alone was used (data not shown).

Anti-PARP p85 Fragment Immunostaining

PARP p85 fragment staining revealed positive cells in the central and peripheral corneal and the bulbar and tarsal conjunctival epithelia and stroma in the treated mice. The punctate and diffuse pattern of PARP staining was similar to that observed in apoptotic liver epithelial cells.[13] The cells showing the strongest staining for PARP in the tarsal conjunctival and central corneal epithelia of treated mice (Fig. 3). In contrast, only nonspecific staining of the conjunctival epithelial basement membrane and weak diffuse cytoplasmic staining was noted in untreated control mice (Fig. 3). No staining was observed in the secondary antibody alone control (data not shown).

Hoechst 33342 Nuclear Staining

Nuclear staining of the cornea and conjunctiva with Hoechst 33342 revealed dysmorphic nuclear architecture and fragmented nuclear material in the treated mice compared with control animals (Fig. 4).

Transmission Electron Microscopy

Ultrastructural nuclear changes consistent with apoptosis were observed in the cornea and conjunctiva of treated mice. Nuclear chromatin condensation and peripheral migration of chromatin, as shown in a representative section in Figure 5, were noted in many conjunctival epithelial cells. These nuclear changes were rarely observed in the conjunctival stromal cells.

Fewer apoptotic cells were noted in the corneal epithelium than in the conjunctiva. Although some nuclear condensation and peripheral margination of chromatin were observed in occasional corneal epithelial cells, nuclear fragmentation to the extent of that in the conjunctival epithelium was not observed.

DISCUSSION

Although apoptosis of ocular surface cells has been detected in chronic dry eye in dogs and humans, our experiments indicate that apoptosis is an acutely inducible event that accompanies the development of KCS in our experimental mouse model of dry eye. Apoptosis on the ocular surface was demonstrated by several markers and by characteristic nuclear morphologic changes. The TUNEL assay revealed DNA fragmentation suggestive of apoptosis in multiple ocular surface tissues, including the central and peripheral corneal epithelium, bulbar and tarsal conjunctival epithelia, tarsal conjunctival stroma, and lid margin in mice with induced dry eye. Immunohistochemistry for caspase 3 and PARP and ultrastructural studies using transmission electron microscopy suggest that the most marked apoptosis occurred in the superficial bulbar conjunctival epithelium. Although TUNEL staining was observed in the peripheral and central corneal epithelium, less ultrastructural evidence of apoptosis was observed at these sites than in the conjunctival epithelial tissues. It is possible that the TUNEL assay may detect cells entering the apoptotic pathway before dissolving into irreversible nuclear fragmentation or it may detect other nonspecific DNA changes induced by ocular surface dryness.

Apoptosis occurs through two pathways, an extrinsic pathway involving the interaction of death ligands (e.g., TNF-α, Fas ligand) with their respective cell surface receptors and an intrinsic pathway that is initiated by insults that damage the DNA, such as ultraviolet light and chemotherapeutic agents. Both pathways eventually result in mitochondrial damage with release of cytochrome *c* and downstream activation of caspases, such as caspase 3. Activation of other downstream caspases results in cleavage of cellular proteins, such as PARP, cytokeratin 18, and other caspases, that lead to the morphologic and biochemical changes of apoptosis (Fig. 6).[14,15]

Poly(ADP-ribose) polymerase (PARP) is a nuclear DNA-binding protein that functions in DNA base excision repair.[16] PARP cleavage results in a decreased enzymatic repair function and contributes to the progression of apoptosis, although PARP

DOCKET ALARM

Explore Litigation Insights

Docket Alarm provides insights to develop a more informed litigation strategy and the peace of mind of knowing you're on top of things.

Real-Time Litigation Alerts

Keep your litigation team up-to-date with **real-time alerts** and advanced team management tools built for the enterprise, all while greatly reducing PACER spend.

Our comprehensive service means we can handle Federal, State, and Administrative courts across the country.

Advanced Docket Research

With over 230 million records, Docket Alarm's cloud-native docket research platform finds what other services can't. Coverage includes Federal, State, plus PTAB, TTAB, ITC and NLRB decisions, all in one place.

Identify arguments that have been successful in the past with full text, pinpoint searching. Link to case law cited within any court document via Fastcase.

Analytics At Your Fingertips

Learn what happened the last time a particular judge, opposing counsel or company faced cases similar to yours.

Advanced out-of-the-box PTAB and TTAB analytics are always at your fingertips.

API

Docket Alarm offers a powerful API (application programming interface) to developers that want to integrate case filings into their apps.

LAW FIRMS
Build custom dashboards for your attorneys and clients with live data direct from the court.

Automate many repetitive legal tasks like conflict checks, document management, and marketing.

FINANCIAL INSTITUTIONS
Litigation and bankruptcy checks for companies and debtors.

E-DISCOVERY AND LEGAL VENDORS
Sync your system to PACER to automate legal marketing.